JOURNAL OF THE AMERICAN COLLEGE OF CARDIOLOGY
PUBLISHED BY ELSEVIER ON BEHALF OF THE AMERICAN
COLLEGE OF CARDIOLOGY FOUNDATION

VOL. 71, NO. 22, 2018

SPECIAL FOCUS ISSUE: CARDIOVASCULAR HEALTH PROMOTION

Coronary Atherosclerotic Precursors of Acute Coronary Syndromes

Hyuk-Jae Chang, MD, PhD,[a] Fay Y. Lin, MD,[b] Sang-Eun Lee, MD, PhD,[a] Daniele Andreini, MD, PhD,[c] Jeroen Bax, MD, PhD,[d] Filippo Cademartiri, MD, PhD,[e] Kavitha Chinnaiyan, MD,[f] Benjamin J.W. Chow, MD,[g] Edoardo Conte, MD,[c] Ricardo C. Cury, MD,[h] Gudrun Feuchtner, MD,[i] Martin Hadamitzky, MD,[j] Yong-Jin Kim, MD,[k] Jonathon Leipsic, MD,[l] Erica Maffei, MD,[m] Hugo Marques, MD,[n] Fabian Plank, MD,[i] Gianluca Pontone, MD, PhD,[c] Gilbert L. Raff, MD,[f] Alexander R. van Rosendael, MD,[d] Todd C. Villines, MD,[o] Harald G. Weirich, MD,[i] Subhi J. Al'Aref, MD,[b] Lohendran Baskaran, MD,[b] Iksung Cho, MD,[a,b,p] Ibrahim Danad, MD,[q] Donghee Han, MD,[a,b] Ran Heo, MD,[r] Ji Hyun Lee, MD,[a,b] Asim Rivzi, MD,[b,s] Wijnand J. Stuijfzand, MD,[b] Heidi Gransar, MSc,[t] Yao Lu, MSc,[b] Ji Min Sung, PhD,[a] Hyung-Bok Park, MD,[a] Daniel S. Berman, MD,[t] Matthew J. Budoff, MD,[u] Habib Samady, MD,[v] Leslee J. Shaw, PhD,[v] Peter H. Stone, MD,[w] Renu Virmani, MD,[x] Jagat Narula, MD, PhD,[y] James K. Min, MD[b]

ABSTRACT

BACKGROUND The association of atherosclerotic features with first acute coronary syndromes (ACS) has not accounted for plaque burden.

OBJECTIVES The purpose of this study was to identify atherosclerotic features associated with precursors of ACS.

METHODS We performed a nested case-control study within a cohort of 25,251 patients undergoing coronary computed tomographic angiography (CTA) with follow-up over 3.4 ± 2.1 years. Patients with ACS and nonevent patients with no prior coronary artery disease (CAD) were propensity matched 1:1 for risk factors and coronary CTA–evaluated obstructive (≥50%) CAD. Separate core laboratories performed blinded adjudication of ACS and culprit lesions and quantification of baseline coronary CTA for percent diameter stenosis (%DS), percent cross-sectional plaque burden (PB), plaque volumes (PVs) by composition (calcified, fibrous, fibrofatty, and necrotic core), and presence of high-risk plaques (HRPs).

RESULTS We identified 234 ACS and control pairs (age 62 years, 63% male). More than 65% of patients with ACS had nonobstructive CAD at baseline, and 52% had HRP. The %DS, cross-sectional PB, fibrofatty and necrotic core volume, and HRP increased the adjusted hazard ratio (HR) of ACS (1.010 per %DS, 95% confidence interval [CI]: 1.005 to 1.015; 1.008 per percent cross-sectional PB, 95% CI: 1.003 to 1.013; 1.002 per mm^3 fibrofatty plaque, 95% CI: 1.000 to 1.003; 1.593 per mm^3 necrotic core, 95% CI: 1.219 to 2.082; all $p < 0.05$). Of the 129 culprit lesion precursors identified by coronary CTA, three-fourths exhibited <50% stenosis and 31.0% exhibited HRP.

CONCLUSIONS Although ACS increases with %DS, most precursors of ACS cases and culprit lesions are nonobstructive. Plaque evaluation, including HRP, PB, and plaque composition, identifies high-risk patients above and beyond stenosis severity and aggregate plaque burden. (J Am Coll Cardiol 2018;71:2511–22) Published by Elsevier on behalf of the American College of Cardiology Foundation.

Listen to this manuscript's audio summary by *JACC* Editor-in-Chief Dr. Valentin Fuster.

From the [a]Division of Cardiology, Severance Cardiovascular Hospital, Integrative Cardiovascular Imaging Research Center, Yonsei University College of Medicine, Seoul, South Korea; [b]Dalio Institute of Cardiovascular Imaging, Department of Radiology, New York-Presbyterian Hospital and Weill Cornell Medicine, New York, New York; [c]Department of Clinical Sciences and Community Health, University of Milan, Centro Cardiologico Monzino, IRCCS, Milan, Italy; [d]Department of Cardiology, Heart Lung Center, Leiden University Medical Center, Leiden, the Netherlands; [e]Cardiovascular Imaging Center, SDN IRCCS, Naples, Italy; [f]Department of Cardiology, William Beaumont Hospital, Royal Oaks, Michigan; [g]Department of Medicine and Radiology, University of Ottawa, Ottawa, Ontario, Canada; [h]Baptist Cardiac and Vascular Institute, Miami, Florida; [i]Department of Radiology, Medical University of Innsbruck, Innsbruck, Austria; [j]Department of Radiology and Nuclear Medicine, German Heart Center Munich, Munich, Germany; [k]Seoul National University College of Medicine, Seoul National University Hospital, Seoul, South Korea; [l]Department of Medicine and Radiology, University of British Columbia, Vancouver, British Columbia, Canada; [m]Department of

ISSN 0735-1097/$36.00 https://doi.org/10.1016/j.jacc.2018.02.079

ABBREVIATIONS AND ACRONYMS

ACS = acute coronary syndrome

CAD = coronary artery disease

CDCC = Clinical and Data Coordinating Center

CI = confidence interval

CL = core laboratory

CTA = computed tomography angiography

DS = diameter stenosis

HRP = high-risk plaque

HU = Hounsfield unit

ICA = invasive coronary angiography

LAP = low-attenuation plaque

NC = necrotic core

PB = plaque burden

PR = positive remodeling

PV = plaque volume

SC = spotty calcification

STEMI = ST-segment elevation myocardial infarction

Prior invasive and pathological studies have identified coronary atherosclerotic plaque features that are central to the pathogenesis of acute coronary syndromes (ACS) (1,2). These include measures of coronary luminal narrowing, plaque burden (PB), arterial remodeling, and plaque composition including thin cap fibroatheroma, necrotic core (NC), and spotty calcification (2–6). However, these findings have been largely derived from atherosclerotic evaluation simultaneous or subsequent to ACS, to partial samples of the coronary artery tree, and to secondary prevention populations (3–5). The utility of vulnerable plaque evaluation in comparison to overall atherosclerotic disease burden has been debated, especially given the technical difficulty of invasive plaque characterization (7).

SEE PAGE 2523

Coronary computed tomography angiography (CTA) is a noninvasive test that enables evaluation of all coronary arteries and their branches in patients with suspected or known coronary artery disease (CAD). The high accuracy of coronary CTA for detection and exclusion of CAD is well reported, and recent advances in computed tomographic technologies now allow for coronary atherosclerotic quantification and characterization, with high diagnostic performance when compared with invasive reference standards (8,9). Limited studies have employed coronary CTA to identify atherosclerotic plaque features associated with ACS (9,10). To date, these studies have used nonstandardized image analysis protocols, nonquantitative methods, mixed populations of patients with and without known CAD, smaller and largely single-center studies, and cohorts with few events (4,9–11).

As coronary CTA is routinely performed in those with suspected but without manifest CAD, it offers a unique opportunity to describe the natural history of atherosclerosis in a primary prevention population of stable patients before ACS occurrence, while accounting for the totality of atherosclerotic features in all coronary arteries and their branches at the patient level (11,12). We aimed to elucidate the prognostic significance of coronary atherosclerosis plaque features for identification of stable patients who will experience future ACS from a nested case-control

Radiology, Area Vasta 1/ASUR Marche, Urbino, Italy; [n]UNICA, Unit of Cardiovascular Imaging, Hospital da Luz, Lisboa, Portugal; [o]Cardiology Service, Walter Reed National Military Center, Bethesda, Maryland; [p]Chung-Ang University Hospital, Seoul, South Korea; [q]VU University Medical Center, Amsterdam, the Netherlands; [r]Asan Medical Center, University of Ulsan College of Medicine, Seoul, South Korea; [s]Department of Radiology, Mayo Clinic, Rochester, Minnesota; [t]Department of Imaging and Medicine, Cedars Sinai Medical Center, Los Angeles, California; [u]Department of Medicine, Los Angeles Biomedical Research Institute, Torrance, California; [v]Division of Cardiology, Emory University School of Medicine, Atlanta, Georgia; [w]Division of Cardiovascular Medicine, Brigham and Women's Hospital, Boston, Massachusetts; [x]CVPath Institute, Gaithersburg, Maryland; and the [y]Icahn School of Medicine at Mount Sinai, Mount Sinai Heart, Zena and Michael A. Wiener Cardiovascular Institute, and Marie-Josée and Henry R. Kravis Center for Cardiovascular Health, New York, New York. This trial was supported by National Institutes of Health Grant HL115150 and the Leading Foreign Research Institute Recruitment Program of the National Research Foundation of Korea, Ministry of Science, ICT & Future Planning. The funders of the study had no role in study design, data collection, data analysis, data interpretation, or writing of the report. Dr. Chang has received funding from the Leading Foreign Research Institute Recruitment Program through the National Research Foundation of Korea funded by the Ministry of Science and ICT (Grant No. 2012027176). Dr. Min has received funding from the National Institutes of Health (grants R01 HL111141, R01 HL115150, R01 118019, and U01 HL 105907), the Qatar National Priorities Research Program (grant 09-370-3-089), and GE Healthcare. Dr. Bax has received unrestricted research grants from Biotronik, Medtronic, Boston Scientific, and Edwards Lifesciences. Dr. Leipsic has served as a consultant for and has stock options in HeartFlow and Circle Cardiovascular Imaging; and has received speaking fees from GE Healthcare. Dr. Chow has received research support from CV Diagnostix; and educational support from TeraRecon Inc. Dr. Pontone has received institutional speaker honoraria and research grants from GE Healthcare, HeartFlow, Medtronic, Bracco, and Bayer. Dr. Raff has received grant support from HeartFlow. Dr. van Rosendael is supported by a research grant from the Netherlands Heart Institute. Dr. Berman has received software royalties from Cedars-Sinai. Dr. Budoff has received grant support from the National Institutes of Health and General Electric. Dr. Samady has received grant support from Phillips, Volcano, St. Jude Medical, Abbott, Medtronic, and Gilead; and has served on the medical advisory board of Volcano and Phillips. Dr. Virmani has received institutional research support from 480 Biomedical, Abbott Vascular, ART, BioSensors International, Biotronik, Boston Scientific, Celonova, Claret Medical, Cook Medical, Cordis, Edwards Lifesciences, Medtronic, MicroVention, OrbusNeich, ReCord, SINO Medical Technology, Spectranetics, Surmodics, Terumo Corporation, W.L. Gore, and Xeltis; has received honoraria from 480 Biomedical, Abbott Vascular, Boston Scientific, Cook Medical, Lutonix, Medtronic, Terumo Corporation, and W.L. Gore; and has served as a consultant for 480 Biomedical, Abbott Vascular, Medtronic, and W.L. Gore. Dr. Min has served as a consultant to HeartFlow; has served on the scientific advisory board of Arineta; has ownership in MDDX; and has a research agreement with GE Healthcare. All other authors have reported that they have no relationships relevant to the contents of this paper to disclose. John Ambrose, MD, served as Guest Editor for this paper.

Manuscript received August 17, 2017; revised manuscript received January 31, 2018, accepted February 6, 2018.

FIGURE 1 CONSORT Diagram for the ICONIC study

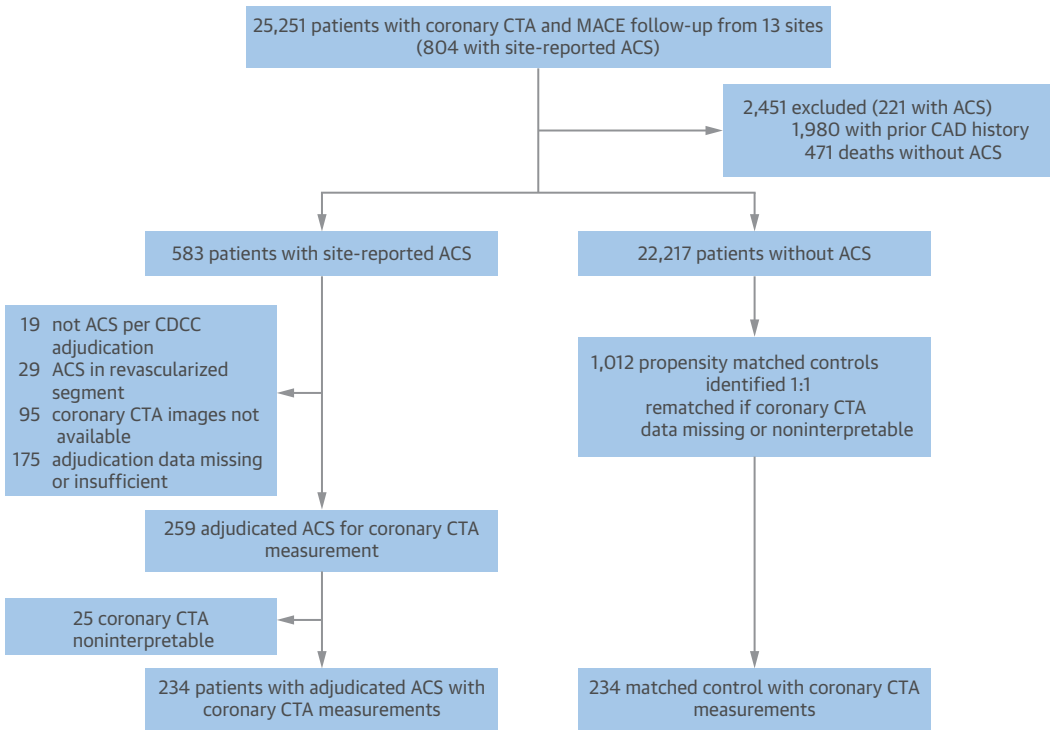

ACS = acute coronary syndrome; CAD = coronary artery disease; CDCC = The Clinical and Data Coordinating Center; CTA = computed tomography angiography; ICONIC = Incident COroNary Syndromes Identified by Computed Tomography; MACE = major adverse cardiac event.

study within a large international multicenter cohort of 25,251 consecutive patients without known CAD undergoing coronary CTA (13).

METHODS

STUDY DESIGN AND STUDY POPULATION. ICONIC (Incident COroNary Syndromes Identified by Computed Tomography) is a nested case-control study of patients without known CAD within the dynamic CONFIRM (Coronary CT Angiography Evaluation for Clinical Outcomes: An International Multicenter) registry, a longitudinal observational cohort study of consecutive individuals undergoing coronary CTA (13). From this registry, 13 sites from 8 countries (the United States, Canada, Germany, Austria, Italy, the Netherlands, Portugal, and South Korea) collected consecutive patients with baseline coronary CTA for a total of 25,416 patients with follow-up for 99.6% over 3.4 ± 2.1 years for all-cause mortality and 95.4% over 3.4 ± 2.1 years for major adverse cardiac events (**Figure 1,** Online Appendix I). Physicians or nurses at each site prospectively collected CAD history, risk factors, and symptoms at the time of baseline coronary CTA; coded coronary CTA stenosis severity by segment; then collected site adjudication of ACS and death. In the present study, patients were eligible if they had no prior CAD, as defined by no prior revascularization or myocardial infarction, and baseline coronary CTA with follow-up of ACS. Patients with deaths without antecedent ACS were censored (**Figure 1**, Online Appendix II). Candidate patients experiencing site-adjudicated ACS were matched 1:1 to within-site control subjects who did not experience ACS. Sites submitted supporting data for ACS as well as baseline coronary CTA images for cases and control subjects. Each site obtained local institutional review board or ethics board approval and submitted study identification-coded data stripped of protected health information for central adjudication and coronary CTA measurement.

The Clinical and Data Coordinating Center (CDCC) at the Dalio Institute of Cardiovascular Imaging performed uniform adjudication of ACS masked to coronary CTA evaluation using definitions set forth by the World Health Organization (WHO) (14). The coronary CTA Core Laboratory (CL) at Severance Hospital of Yonsei University performed comprehensive and

quantitative analysis of coronary CTAs blinded to case status. The final study population consisted of CDCC-adjudicated ACS and their paired within-site control subjects that had coronary CTA-CL-measured baseline coronary CTA.

Among 25,251 patients with follow-up for major adverse cardiac events (804 site-reported ACS, 3.2%) at 13 sites over 3.4 ± 2.1 years, 2,451 patients (221 site-reported ACS) were excluded for prior CAD or death without ACS, leaving 22,800 (583 site-reported ACS) eligible for the study. After exclusion of site-reported ACS with insufficient or absent clinical data (n = 181), with ACS in an interval revascularized coronary segment (n = 29), with adjudication by the CDCC as not meeting criteria for ACS (n = 19), without coronary CTA data to submit to the CL (n = 95), or with coronary CTA data that was not interpretable for CL measurements (n = 25), the final ICONIC study cohort comprised 234 ACS cases and 234 propensity-matched control subjects (**Figure 1**).

PROPENSITY SCORE MATCHING. Matching factors were determined a priori, and all variables forced into propensity scoring using logistic regression were used to predict ACS in the main model. Factors entered into propensity scoring procedures included age, male sex, hypertension, hyperlipidemia, diabetes mellitus, family history of premature CAD, current smoking, and CAD severity assessed by coronary CTA, defined as nonobstructive, 1-vessel, 2-vessel, or 3-vessel/left main disease at the 50% diameter stenosis threshold (area under the receiver-operating curve 0.94, 95% confidence interval [CI]: 0.92 to 0.95) (Online Appendix III). A nearest-neighbor approach using 1:1 matching was performed on site, and propensity score with a greedy matching technique was used to match all cases. Relaxed models for missing variables were utilized to allow all cases to be matched regardless of missing data (15).

ACS EVENT ADJUDICATION. The CDCC reviewed ACS event data including cardiac enzyme measurement, electrocardiograms, and invasive coronary angiograms (ICAs) blinded to coronary CTA data, and adjudicated ACS using the World Health Organization's MONICA (Multinational MONItoring of trends and determinants in CArdiovascular disease) universal definition of myocardial infarction (Online Appendix IV) (14,16). For ACS cases that underwent ICA at the time of ACS, 1 culprit lesion per patient was adjudicated blinded to coronary CTA data using the modified ROMICAT (Rule Out Myocardial Infarction/Ischemia Using Computer-Assisted Tomography II) definition and coded using a modified Society of Cardiovascular Computed Tomography (SCCT) 18-segment coronary tree (Online Appendix V) (11). ACS cases with culprit lesions in interval revascularized segments were excluded.

Among 234 patients with adjudicated ACS, 32 patients were excluded for absence of ICA performance, 26 patients were excluded for unavailable ICA to adjudicate a culprit lesion, and 14 patients underwent ICA with no culprit lesion that could be determined, leaving 162 patients with adjudicated culprit lesions. The 72 ACS cases without adjudicated culprits did not differ from the 162 cases with adjudicated culprits in age, sex, and type of ACS, but did exhibit fewer lesions and lesser %DS (Online Table VII-4).

BASELINE CORONARY CTA ANALYSIS. Baseline coronary CTA performance and site interpretation was performed using computed tomography scanners of ≥64-detector rows in direct accordance with SCCT guidelines (12,17). The coronary CTA-CL analyzed site-submitted Digital Imaging and Communications in Medicine files masked to clinical results and case status. Independent level III-experienced readers at the coronary CTA-CL performed standardized measurements using semiautomated plaque analysis software (QAngioCT Research Edition version 2.1.9.1, Medis Medical Imaging Systems, Leiden, the Netherlands) (**Central Illustration**) with appropriate manual correction (18).

Briefly, for each segment of the 18-segment SCCT model with a diameter ≥2 mm (Online Appendix VI), quantitative analysis was performed on every 1-mm cross-section to measure vessel length, volume, plaque volume (PV), mean PB, and plaque composition using pre-defined Hounsfield unit (HU) thresholds: NC (−30 to 30 HU), fibrofatty (30 to 130 HU), fibrous (131 to 350 HU), and calcified plaque (≥350 HU) (12,19). The interobserver and intraobserver intraclass correlations for total PV were 0.992 and 0.996, respectively ($p < 0.001$). The interobserver and intraobserver intraclass correlation for plaque composition ranged from 0.95 to 0.99 (Online Table VI-1).

Additionally, for each lesion, measurements were performed of length, volume, and plaque composition, as well as percent diameter stenosis (%DS), area stenosis, minimum luminal diameter, minimum luminal area, cross-sectional PB, mean PB, and remodeling index (Online Appendix VI) (20). Cutpoints of ≥50% and ≥70% %DS were used for obstructive CAD. Binary evaluation of adverse plaque characteristics included positive remodeling (PR), low attenuation plaque (LAP), spotty calcification (SC), bifurcation, and tortuosity. High-risk plaque (HRP) was defined as the presence within a coronary lesion of ≥2 features including PR, LAP, or SC (9,10). Segment-based PVs and lesion-based measurements were summarized to the patient level, and diffuseness of atherosclerosis

CENTRAL ILLUSTRATION **Precursors of Acute Coronary Syndrome and Control Subjects as Identified by Coronary CTA**

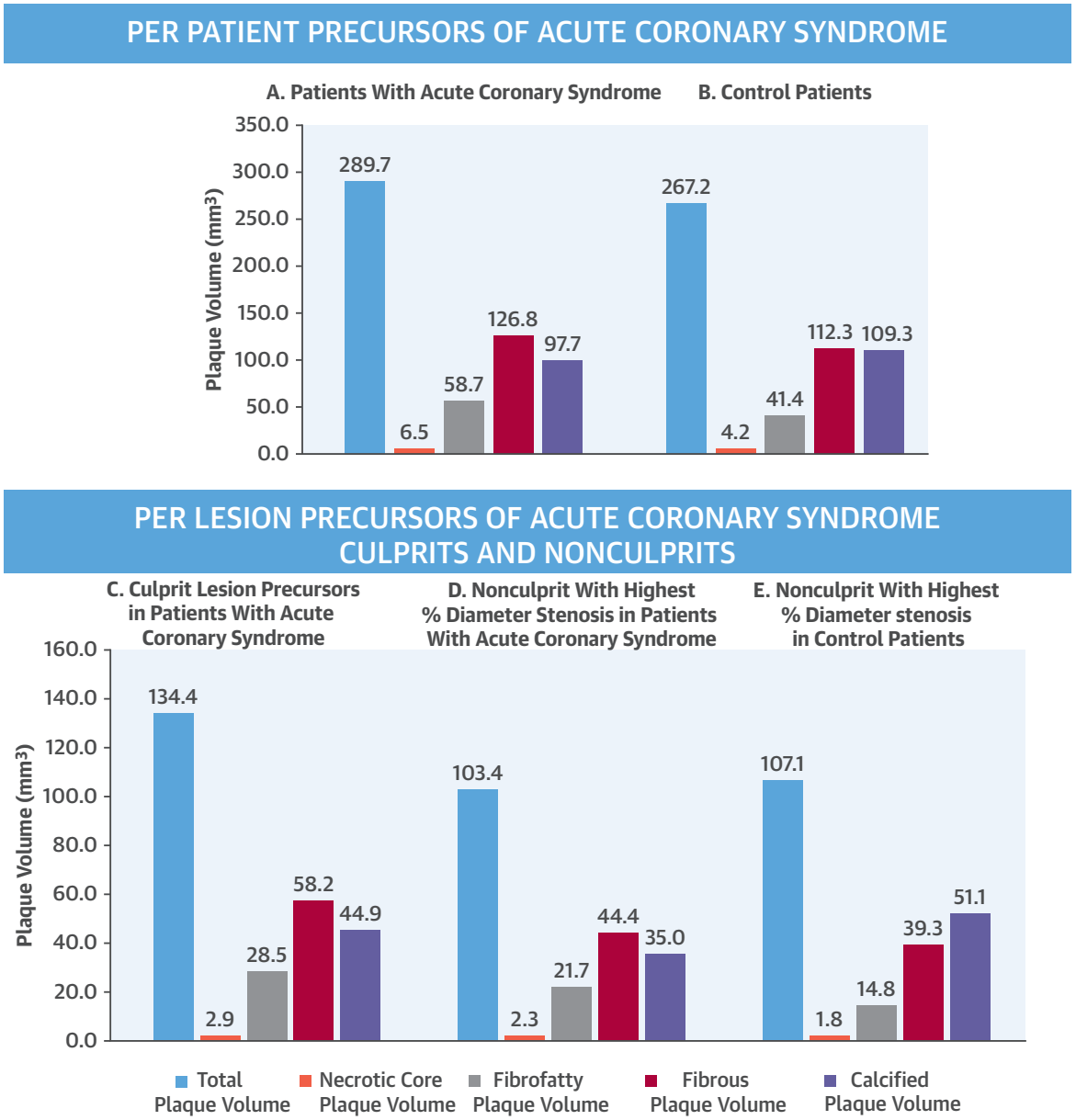

Chang, H.-J. et al. J Am Coll Cardiol. 2018;71(22):2511–22.

(A) Adjudicated first ACS cases with coronary CTA measurements (n = 234) of a nested case-control cohort of 25,251 patients undergoing coronary CTA exhibit elevated fibrofatty and necrotic core volumes (65.2 ± 95.4 mm^3); 34.6% exhibit diameter stenosis ≥50%, and 52.1% exhibit high-risk plaque. **(B)** Nonevent control subjects propensity matched by demographics, risk factors, and number of obstructive vessels by coronary CTA exhibit lesser fibrofatty and necrotic core volumes (45.6 ± 68.8, multivariate adjusted p = 0.008) with no difference in calcified or total plaque volumes (p = NS for all); %DS and HRP are significantly decreased in control patients (p <0.05 for all). **(C)** Culprit lesion precursors exhibit elevated fibrofatty and necrotic core volumes (31.32 ± 55.5 mm^3). **(D)** Within-patient controls, using the nonculprit with the highest baseline %DS, exhibit lesser total plaque and necrotic core volumes (p <0.05 for both). **(E)** Between-patient controls, using the lesion with the highest % DS in the control patient, exhibit lesser non-calcified plaque components (p = 0.04), but no decrease in calcified plaque volume (p = NS). ACS = acute coronary syndrome; coronary CTA = coronary computed tomographic angiography; %DS = percent diameter stenosis; HRP = high-risk plaque; NS = nonsignificant.

was calculated as the ratio of summed lesion lengths and total vessel length.

Subsequent to coronary CTA-CL analysis, ICA-identified culprit lesions were coregistered to the baseline coronary CTA precursor lesions (D.H., F.Y.L.) by comparison of coronary segment coding and using distance from ostia and coronary vessel branch points as fiduciary landmarks. Unblinded comparison of ICA and coronary CTA was allowed for alignment of lesions but not for reclassification of ACS.

STATISTICAL ANALYSIS. At the patient level, patients with ACS were compared 1:1 to matched patients who did not experience ACS. At the lesion level, culprit lesion precursors were compared: 1) within-subject, to all remaining nonculprit lesions in the same ACS patient; 2) within-subject, to the nonculprit lesion with the highest %DS in the same ACS patient; and 3) between-subject, to the lesion with the highest %DS in the paired control non-ACS patient.

Continuous variables are expressed as mean ± SD, and categorical variables are presented as absolute counts and percentages. Differences between categorical variables were analyzed using McNemar's test or chi-square test, as appropriate, and those between continuous variables using paired the Wilcoxon rank sum test.

Multivariate marginal Cox models adjusting for conventional clinical risk factors were used to compare atherosclerotic plaque differences accounting for propensity matching between case and control subjects (21). The robust variance estimator accounts for the clustering within matched pairs. For per-lesion level analysis, marginal Cox regression was used to account for patient effects (22,23). Components of the propensity score were not candidates for multivariate regression.

A p value <0.05 was considered to indicate a statistically significant difference. All analyses were performed with SAS version 9.4 (SAS Institute Inc., Cary, North Carolina) and R version 3.3.0 (R Foundation for Statistical Computing, Vienna, Austria).

RESULTS

BASELINE PATIENT CHARACTERISTICS AND CLINICAL EVENTS. The final ICONIC study cohort comprised 234 CDCC-adjudicated ACS cases and 234 propensity-matched control subjects with coronary CTA-CL-measured baseline coronary CTA. The average age of the nested case-control cohort was 62.2 ± 11.5 years (63% male) with follow-up time of 3.9 ± 2.5 years. ACS and control patients were well matched by propensity score (0.07 ± 0.04 vs. 0.07 ± 0.04; $p = 0.73$). ACS cases had lower rates of diabetes mellitus, a component of the propensity score (19.7% vs. 31.6%; $p < 0.001$), and greater angina severity ($p = 0.004$) (Online Appendix VII). Otherwise, there were no differences in baseline clinical risk factors, medications, and lipid profiles.

ACS events comprised 40 ST-segment elevation myocardial infarctions (STEMIs), 114 non-STEMIs, 6 myocardial infarctions wherein STEMI and non-STEMI could not be distinguished due to the timing of electrocardiogram relative to the ACS, and 74 cases of unstable angina pectoris. Culprit lesion precursors were identified by both ICA and baseline coronary CTA in 129 (53.4%) patients. During follow-up, patients with ACS more frequently experienced interval revascularization between baseline coronary CTA and last follow-up than control subjects (50.4% vs. 23.5%; $p < 0.001$), and the time to interval revascularization was shorter in patients with ACS, with a median of 26 days (interquartile range [IQR]: 5 to 312 days) compared with 64 days (IQR: 19 to 199 days; $p = 0.03$).

PER-PATIENT BASELINE CORONARY CTA FINDINGS IN ACS AND CONTROL PATIENTS. Overall, there were an average of 3.9 ± 2.5 lesions in patients with ACS and 3.7 ± 2.7 lesions in control subjects ($p = 0.40$) (Table 1). The maximal %DS at the per-patient level was <50% for both patients with ACS and control subjects (44.2 ± 26.4% vs. 33.7 ± 22.0%; $p < 0.001$), with case and control subjects exhibiting >50% stenosis in 34.6% versus 19.2% and >70% stenosis in 12.8% versus 5.1%, respectively.

Patients with ACS did not differ significantly from control subjects in total PV (289.7 ± 308.4 mm^3 vs. 267.2 ± 285.7 mm^3; $p = 0.321$), calcified PV (97.7 ± 136.1 mm^3 vs. 109.3 ± 164.0 mm^3; $p = 0.389$), or fibrous PV (126.8 ± 131.6 mm^3 vs. 41.4 ± 62.2 mm^3; $p = 0.137$), but had significantly higher fibrofatty (58.7 ± 85.8 mm^3 vs. 41.4 ± 62.2 mm^3; $p = 0.009$) and NC volumes (6.5 ± 14.0 mm^3 vs. 4.2 ± 8.8 mm^3; $p = 0.026$). These findings remained consistent when PVs were normalized to vessel volume. The maximal cross-sectional PB was also significantly higher in cases than control subjects (66.1 ± 25.8% vs. 56.5 ± 28.7%; $p < 0.001$), with no significant difference in the mean PB.

Patients with ACS exhibited HRP more frequently than control subjects (52.1% vs. 33.3%; $p = 0.003$) in addition to each component of HRP, including LAP, PR, and SC (all $p < 0.05$). Patients with ACS exhibited greater atherosclerotic plaque diffuseness, but did not differ from control subjects in atherosclerotic plaques at sites of vessel bifurcation or at tortuous points within the vessel (all $p > 0.05$).

PER-PATIENT BASELINE ATHEROSCLEROTIC PLAQUE PRECURSORS OF ACS EVENTS. In marginal Cox

regression analysis adjusting for angina severity and interval revascularization, highest %DS severity was an indicator of future adverse events (HR: 1.010 for every 1% increase in stenosis; 95% CI: 1.005 to 1.015; p = 0.002), as well as the presence of high-grade coronary stenosis ≥70% (HR: 1.536; 95% CI: 1.141 to 2.067; p = 0.005 (Table 2).

At the patient level, neither total PV nor mean PB was associated with an increased hazard of ACS occurrence (all p > 0.05). However, fibrofatty, NC plaque, and the sum of both were significant predictors for ACS (For every 1 mm^3 increase respectively, HR: 1.002, 95% CI: 1.000 to 1.004, p = 0.048; HR: 1.013, 95% CI: 1.003 to 1.022, p = 0.009; and HR: 1.002, 95% CI: 1.000 to 1.003; p = 0.037). Calcified and fibrous PVs were not associated with ACS (all p > 0.05). The maximal cross-sectional PB was also significantly associated with ACS (HR: 1.008 for every %; 95% CI: 1.003 to 1.013; p = 0.003).

The presence of HRP was associated with ACS (HR: 1.593; 95% CI: 1.219 to 2.082; p = 0.001), as were its constituents LAP (HR: 1.378; 95% CI: 1.051 to 1.805; p = 0.020) and SC (HR: 1.543; 95% CI: 1.169 to 2.037; p = 0.002). PR trended toward association with ACS (p = 0.085).

PER-LESION BASELINE ATHEROSCLEROTIC PLAQUE PRECURSORS OF ACS CULPRIT LESIONS. Of the 162 patients with ICA available for culprit lesion adjudication, there were 129 cases where the culprit lesion by ICA could be aligned to a baseline lesion by coronary CTA with lesion measurements. The duration of time between baseline coronary CTA and follow-up ICA was a median of 0.08 years (IQR: 0.008 to 1.42 years). In 21 cases, the culprit lesion aligned to normal segments on the baseline coronary CTA with no lesion measurements, and in the remaining 12 patients, the baseline lesion by coronary CTA could not be measured due to artifact or small vessel size. More than three-quarters of the 129 culprit lesion precursors exhibited <50% stenosis in the baseline coronary CTA (38.27 ± 20.97%), with relatively long lesions (35.90 ± 21.66 mm) (Table 3). Overall PV was 134.4 ± 141.5 mm^3, which comprised 44.88 ± 60.29 mm^3, 58.22 ± 62.39 mm^3, 28.47 ± 50.18 mm^3, and 2.85 ± 9.27 mm^3 of calcified, fibrous, fibrofatty, and NC volume, respectively (Central Illustration). The cross-sectional PB was elevated (62.54 ± 22.38). HRP was observed in 31.01% of culprit lesion precursors, and 24.03%, 76.74%, and 17.83% of culprit lesion precursors possessed LAP, PR, and SC, respectively.

Compared with within-subject nonculprit lesions, culprit-lesion precursors exhibited elevated hazard for greater %DS (HR: 1.023 per % increase; 95% CI: 1.015 to 1.031; p < 0.001), lesion length (HR: 1.021 per mm of length; 95% CI: 1.013 to 1.029; p < 0.001), PV (HR: 1.002 per mm^3 of volume; 95% CI: 1.001 to 1.003; p < 0.001) and all plaque constituents (p < 0.001 for all), notably fibrofatty and NC volume (HR: 1.007 per mm^3; 95% CI: 1.003 to 1.010; p < 0.001). Culprit lesions also exhibited elevated hazard for cross-sectional PB (HR: 1.027 per % increase; 95% CI: 1.018 to 1.035; p < 0.001); HRP (HR: 1.954; 95% CI: 1.317 to 2.899; p = 0.001), LAP (HR: 1.805; 95% CI: 1.198 to 2.721; p = 0.005), and SC (HR: 1.702; 95% CI: 1.064 to 2.722; p = 0.026). Comparison to between-subject

TABLE 1 Coronary CTA Findings in Patient-Level Analysis

Atherosclerotic Feature	ACS (n = 234)	Control (n = 234)	p Value
Number of total lesions	3.9 (2.5)	3.7 (2.7)	0.400
%DS	44.2 ± 26.4	33.7 ± 22.0	<0.001
%DS ≥50%	81 (34.6)	45 (19.2)	<0.001
%DS ≥70%	30 (12.8)	12 (5.1)	0.007
Area stenosis, %	61.9 ± 27.2	51.2 ± 27.9	<0.001
Minimum luminal area, mm^2	2.3 ± 2.1	2.6 ± 1.9	0.014
Minimum luminal diameter, mm	1.3 ± 0.7	1.5 ± 0.6	0.004
CAD severity by number of vessels			0.020
None	15 (6.4)	34 (14.5)	
Nonobstructive (≤50% DS)	104 (44.4)	91 (38.9)	
1-vessel disease	69 (29.5)	59 (25.2)	
2-vessel disease	25 (10.7)	21 (9.0)	
3-vessel/left main disease	21 (9.0)	29 (12.4)	
Total plaque volume, mm^3	289.7 ± 308.4	267.2 ± 285.7	0.321
Calcified, mm^3	97.7 ± 136.1	109.3 ± 164.0	0.389
Fibrous, mm^3	126.8 ± 131.6	112.3 ± 119.3	0.137
FF, mm^3	58.7 ± 85.8	41.4 ± 62.2	0.009
NC, mm^3	6.5 ± 14.0	4.2 ± 8.8	0.026
FF + NC, mm^3	65.2 ± 95.4	45.6 ± 68.8	0.008
Noncalcified, mm^3	192.0 ± 207.8	157.9 ± 173.6	0.030
Composition by % vessel volume			
% Calcified	4.1 ± 5.9	4.5 ± 6.2	0.709
% Fibrous	5.2 ± 4.6	4.5 ± 6.2	0.067
% FF	2.3 ± 3.0	1.7 ± 2.5	0.011
% NC	0.3 ± 0.7	0.2 ± 0.4	0.039
% FF + NC	2.6 ± 3.5	1.9 ± 2.7	0.012
% Noncalcified volume	7.8 ± 7.2	6.5 ± 6.7	0.020
Mean plaque burden, %	11.9 ± 10.9	11.0 ± 10.7	0.152
Max cross-sectional plaque burden, %	66.1 ± 25.8	56.5 ± 28.7	<0.001
Diffuseness, %	25.8 ± 19.4	22.3 ± 19.2	0.030
Adverse plaque characteristics			
Bifurcation, no. of lesions	2.3 ± 1.6	2.1 ± 1.7	0.218
Tortuous vessels, no. of lesions	0.08 ± 0.34	0.05 ± 0.28	0.477
High-risk plaque present	122 (52.1)	78 (33.3)	0.003
Low-attenuation plaque present	101 (43.2)	64 (27.4)	<0.001
Positive remodeling present	205 (87.6)	187 (79.9)	0.026
Spotty calcification present	72 (30.8)	47 (20.1)	0.013

Values are n (%) or mean ± SD.

ACS = acute coronary syndrome; CAD = coronary artery disease; CTA = computed tomography angiography; DS = diameter stenosis; FF = fibrofatty; NC = necrotic core.

TABLE 2 Per-Patient Multivariate Marginal Cox Model Predicting Acute Coronary Syndrome

Atherosclerotic Feature	HR (95% CI)*	p Value
Highest % diameter stenosis severity, per %	1.010 (1.005–1.015)	0.002
Presence of ≥50% diameter stenosis	1.437 (0.948–2.179)	0.088
Presence of ≥70% diameter stenosis	1.536 (1.141–2.067)	0.005
Plaque volume, per mm^3	1.000 (0.999–1.000)	0.792
Calcified	0.999 (0.998–1.000)	0.092
Fibrous	1.000 (0.999–1.001)	0.941
FF	1.002 (1.000–1.004)	0.048
NC	1.013 (1.003–1.022)	0.009
FF and NC	1.002 (1.000–1.003)	0.037
Noncalcified	1.000 (1.000–1.001)	0.352
Mean plaque burden, %	1.005 (0.997–1.013)	0.209
Max cross-sectional plaque burden, %	1.008 (1.003–1.013)	0.003
Diffuseness, per %	1.146 (0.622–2.111)	0.662
High-risk plaque present	1.593 (1.219–2.082)	0.001
Low-attenuation plaque present	1.378 (1.051–1.805)	0.020
Positive remodeling present	1.401 (0.955–2.056)	0.085
Spotty calcification present	1.543 (1.169–2.037)	0.002

*Adjusted for angina severity and interval revascularization.
CI = confidence interval; HR = hazard ratio; other abbreviations as in Table 1.

control lesions with highest %DS and to within-subject nonculprits with highest %DS demonstrated a consistent attenuation of the association with %DS, calcified PV, and fibrous PV ($p > 0.05$ for all). Total PV, mean PB, fibrofatty and NC volume, and HRP exhibited elevated hazards with variable statistical significance depending upon the choice of control.

DISCUSSION

In this nested case-control study from a large prospective multinational registry of patients undergoing coronary CTA, we observed measures of coronary luminal narrowing to be associated with but generally imprecise discriminators of future ACS. At the patient level, only 34.6% possessed a coronary lesion with ≥50% diameter stenosis prior to ACS, with only 12.8% exhibiting ≥70% stenosis. These findings were further accentuated at the lesion level, wherein precursor lesions of culprit plaques were identified as causing ≥50% and ≥70% luminal obstruction only 24.8% and 4.7% of the time, respectively.

One major limitation of the extant literature on vulnerable plaque characterization is that its predictive value has not accounted for the denominator of atherosclerotic disease burden in the vulnerable patient (7,24). Our study fills an important knowledge gap as case and control patients were propensity matched for major patient-level characteristics including clinical risk factors and number of obstructive coronary vessels, and did not differ by total PV or mean PB. We observed that lesion morphology, inclusive of cross-sectional PB, HRP, LAP, PR and SC, and PB by composition, had independent predictive value for ACS, above and beyond clinical risk factors and total atherosclerotic disease burden.

Our per-lesion level results underline the complementary importance of atherosclerotic disease burden in relation to plaque morphology and composition. In unmatched analyses, culprit lesion precursors compared with other lesions within case patients displayed increased PV, greater length, as well as greater %DS, cross-sectional PB, composition-specific PVs, and prevalence of HRP. When compared to between-patient control lesions or within-patient nonculprit lesions with the highest luminal narrowing, the association with calcified and fibrous PVs was weakened. Thus, atherosclerotic PB is an important marker of lesions at risk, but controlling for PB, there is independent prognostic value of plaque features and composition. Additionally, within a single patient or compared with a control, future culprit lesions share many common features with baseline stenotic lesions, but the presence of lesions with high-risk plaque features and fibrofatty or NC demarcate risk on a per-lesion and -patient level.

Our results confirm the findings of prior landmark studies using invasive coronary angiography, demonstrating that although %DS is a strong indicator of future adverse events, only a minority of ACS culprit lesion precursors cause significant coronary artery luminal narrowing prior to ACS occurrence, even with a shorter duration between baseline coronary CTA and ICA (25,26). Our results additionally confirm the association of ACS with findings posited by pathological and invasive imaging studies, including PVs, necrotic and fibrofatty plaque compositions, and HRP features (3,5). In PROSPECT (Providing Regional Observations to Study Predictors of Events in the Coronary Tree) the sole multicenter prospective study of vulnerable plaque characteristics to date, among patients undergoing a repeat percutaneous coronary intervention in nearly all cases for increasing angina as their clinical presentation, the baseline intravascular ultrasound predictors of future ACS included minimum luminal area, cross-sectional PB, and thin cap fibroatheroma (5,27). Our study found congruent results with %DS, cross-sectional PB, and HRP findings associated with thin cap fibroatheroma including LAP (28). Our study findings extend the scope of these pathological and invasive studies to a primary prevention population, with ACS rather than angina outcomes, and using a matched case-control population wherein differences

TABLE 3 Lesion-Level Analysis for Identification of Culprit Lesion Precursors

	Culprit Lesion Precursor (n = 129)	Within-Patient All Nonculprits in Patients With ACS (n = 479)			Within-Patient Nonculprit With Highest %DS in Patients With ACS (n = 118)*			Between-Patient Lesion With Highest %DS in Control Patients (n = 129)		
			HR† (95% CI)	p Value		HR† (95% CI)	p Value		HR† (95% CI)	p Value
%DS	38.27 ± 20.97	26.23 ± 18.02	1.023 (1.015–1.031)	<0.001	42.64 ± 22.23	1.002 (0.994–1.011)	0.612	37.04 ± 20.63	1.001 (0.992–1.010)	0.898
%DS ≥50%	32 (24.81)	41 (6.68)	2.813 (1.736–4.558)	<0.001	31 (26.27)	1.256 (0.796–1.982)	0.328	27 (20.93)	1.086 (0.682–1.729)	0.727
%DS ≥70%	6 (4.65)	11 (1.25)	1.717 (0.678–4.350)	0.254	11 (9.32)	0.607 (0.227–1.622)	0.319	8 (6.20)	0.684 (0.268–1.746)	0.427
Lesion length, mm	35.90 ± 21.66	23.71 ± 15.90	1.021 (1.013–1.029)	<0.001	30.55 ± 17.63	1.010 (1.001–1.018)	0.029	29.36 ± 21.71	1.004 (0.997–1.011)	0.225
Plaque volume, mm^3	134.4 ± 141.50	61.75 ± 113.07	1.002 (1.001–1.003)	<0.001	103.44 ± 160.55	1.001 (1.000–1.002)	0.030	107.11 ± 125.80	1.000 (0.999–1.002)	0.590
Calcified	44.88 ± 60.29	21.18 ± 45.78	1.004 (1.001–1.006)	0.002	35.0 ± 56.89	1.002 (1.000–1.004)	0.077	51.07 ± 83.89	0.998 (0.996–1.001)	0.137
Fibrous	58.22 ± 62.39	27.49 ± 46.47	1.005 (1.002–1.007)	<0.001	44.38 ± 60.78	1.002 (0.999–1.005)	0.108	39.31 ± 47.11	1.002 (0.999–1.005)	0.154
FF	28.47 ± 50.18	11.99 ± 34.08	1.007 (1.003–1.010)	<0.001	21.71 ± 55.67	1.003 (0.999–1.007)	0.124	14.80 ± 26.29	1.006 (1.002–1.010)	0.006
NC	2.85 ± 9.27	1.09 ± 4.20	1.029 (1.018–1.040)	<0.001	2.28 ± 6.86	1.014 (1.001–1.027)	0.042	1.75 ± 4.71	1.012 (1.002–1.022)	0.021
FF and NC	31.32 ± 55.5	13.08 ± 37.28	1.006 (1.003–1.009)	<0.001	23.99 ± 60.5	1.003 (0.999–1.007)	0.119	16.55 ± 29.96	1.005 (1.001–1.008)	0.006
Noncalcified	89.51 ± 107.36	40.55 ± 77.27	1.003 (1.002–1.005)	<0.001	68.34 ± 114.82	1.002 (1.000–1.003)	0.066	55.85 ± 67.15	1.002 (1.000–1.004)	0.042
Mean plaque burden, %	27.12 ± 13.40	19.67 ± 11.5	1.045 (1.032–1.059)	<0.001	24.52 ± 11.36	1.028 (1.011–1.045)	0.001	25.42 ± 14.75	1.003 (0.989–1.017)	0.680
Max plaque burden, %	62.54 ± 22.38	50.70 ± 20.38	1.027 (1.018–1.035)	<0.001	63.24 ± 21.31	1.008 (1.000–1.016)	0.050	57.84 ± 27.83	1.003 (0.996–1.010)	0.415
High-risk plaque	40 (31.01)	95 (19.83)	1.954 (1.317–2.899)	0.001	36 (30.51)	1.239 (0.841–1.827)	0.279	23 (17.83)	1.542 (1.105–2.153)	0.011
Low-attenuation plaque	31 (24.03)	68 (14.20)	1.805 (1.198–2.721)	0.005	28 (23.73)	1.085 (0.696–1.693)	0.718	22 (17.05)	1.223 (0.840–1.780)	0.294
Positive remodeling	99 (76.74)	379 (79.12)	1.048 (0.675–1.628)	0.835	87 (73.73)	1.202 (0.743–1.946)	0.453	73 (56.59)	2.031 (1.306–3.160)	0.002
Spotty calcification	23 (17.83)	62 (12.94)	1.702 (1.064–2.722)	0.026	18 (15.25)	1.506 (0.955–2.375)	0.078	13 (10.08)	1.763 (1.241–2.503)	0.002

Values are mean ± SD or n (%), unless otherwise indicated. *Eleven patients had measurements only for the culprit lesion and lacked a within-patient comparator. †Adjusted for angina severity and interval revascularization.

Abbreviations as in Tables 1 and 2.

in coronary luminal and atherosclerotic plaque features would be expectedly causal to the event (5,27). Finally, in the largest international multicenter cohort of patients with ACS, our results demonstrate the prognostic value and generalizability of noninvasive plaque evaluation across a broad array of countries, coronary CTA scanners, and protocols, and strengthens prior observations with invasive studies in that the majority of our outcome events were myocardial infarctions, and not unstable or increasing angina.

Prior coronary CTA studies have similarly evaluated the importance of atherosclerotic plaque features for prognosticating ACS. Limited to single centers, these studies have nevertheless highlighted the benefit of morphological coronary assessment of LAP, PR, and SC (4,9,10). Our study extends these pioneering studies by demonstrating the predictive value of noninvasive plaque quantitation by composition as well as morphology. We also highlight the significance of cross-sectional PB in coronary CTA evaluation, which has previously been emphasized only in the published invasive imaging data.

Our observation of gradations of risk within categories of noncalcified plaque, most notably for fibrofatty and necrotic volumes, integrates the published data correlating coronary CTA plaque composition with pathology and invasive imaging. Current-generation coronary CTA lacks the spatial resolution to visualize fibrous cap thickness to characterize thin cap fibroatheroma; hence, coronary CTA plaque evaluation must rely on methods that focus on luminal, vessel remodeling, and plaque composition using HU thresholds, such as HU <30, that are

associated with NC, and morphological HRP criteria such as LAP, SC, and PR that are associated with thin cap fibroatheroma (28,29). Thresholds for calcium, NC, and intermediate degrees of fibrous tissue have largely been validated against virtual histology-intravascular ultrasound, but against the gold standard of histopathology, the HU of NC and fibrous plaque demonstrates significant overlap (19,30). Conversely, the low risk of calcified plaque is consistent with virtual histology-intravascular ultrasound studies demonstrating that transformation of noncalcified plaques to calcified plaques is associated with a more benign prognosis (31). The implication for coronary CTA patient evaluation is that there is a continuum of risk by plaque composition, with greater weight for lower-attenuation PB than calcified or higher-attenuation noncalcified plaque.

Taken together, the aforementioned findings allow several conclusions to be drawn at both the lesion and patient level. First, coronary luminal narrowing is a prognostic indicator of future ACS, but a threshold of ≥50% has low sensitivity for patients and lesions that will result in ACS, highlighting the need for additional or improved markers of risk. Furthermore, the present data support that within a patient, the lesion with greatest overall PV as well as fibrofatty and NC PV has the greatest probability of becoming a culprit ACS lesion, not necessarily the one displaying the highest %DS. From the results of this study, when aiming to discriminate a patient with or without risk of ACS, it appears essential to integrate atherosclerosis feature findings with consideration of PV and presence of HRPs. Second, consistent with the dynamic nature of HRP and the frequent observation of clinically silent healed ruptures, we observed a relatively low sensitivity of HRP of 69% to predict a culprit lesion on a per-lesion basis, with a higher sensitivity on a per-patient basis. We posit that atherosclerotic plaque features represent a dimension of disease burden that may better identify at-risk patients on a whole patient basis. That is, individual plaque imaging may signal more information about the patient than about the individual lesion or the total PB alone. Finally, we observed that in 21 of the 162 patients with ICA available, the culprit lesion aligned to normal segments on the baseline coronary CTA. This may represent baseline nonobstructive plaque below the spatial resolution of coronary CTA, interval rapid plaque progression, or mechanisms of acute coronary events other than plaque rupture, such as plaque erosion. Our study design did not prescribe repeat coronary CTA, but prospective studies with serial coronary CTA are needed to address plaque progression in previously normal segments.

STUDY LIMITATIONS. First, as they are derived from a large observational cohort study, the present findings are susceptible to unmeasured confounding factors, referral bias, and potential biases in propensity-matched control subjects. Indications for coronary CTA were for evaluation of CAD in clinically stable patients, as the CONFIRM registry included many patients from non-U.S. sites and with coronary CTAs prior to the introduction of appropriate use criteria. However, use of the existing cohort study allowed collection of the largest international multicenter cohort of atherosclerotic plaque precursors to ACS to date. Second, to ensure proper adjudication of ACS events, we censored patients who died without confirmatory findings of ACS. Thus, these findings should be considered limited to patients at risk of experiencing nonfatal ACS, and future studies should investigate whether the present findings apply to fatal ACS. Missing adjudication data may also contribute to information bias. Third, propensity score matching on the likelihood of ACS results in well-matched control subjects with complete and careful coronary CTA measurements, but reduces generalizability to the general pool of patients undergoing coronary CTA (Online Appendix VIII). Prediction models will require prospective cohorts in a generally low-risk population and, given the time and costs of quantitative computed tomography, may be economically feasible only with completely automated coronary CTA measurements or deep learning. Fourth, atherosclerotic quantification and characterization was performed only on a single baseline coronary CTA. Thus, information related to atherosclerosis progression or transformation as related to time to ACS occurrence remains unknown.

CONCLUSIONS

Despite advances in risk stratification, ACS remains burdensome and unpredictable, and an integrated evaluation of vulnerable plaque identifies the vulnerable patient above and beyond the clinical risk factors and aggregate PB. In this multicenter case-control study of stable patients without known CAD, the majority did not possess high-grade coronary stenosis before experiencing ACS. Coronary atherosclerotic precursors of ACS exhibited elevated fibrofatty and NC volumes, but not total or calcified volumes. HRP and its features of LAP, PR, and SCs, as well as cross-sectional PB, also identified lesions and patients that will experience ACS. Perhaps of greatest import, the atherosclerotic plaque features that contribute to

a coronary stenosis, rather than just the stenosis itself, contribute robust incremental prognostic information both on a per-plaque and a per-patient basis. Our data suggest a potential paradigm shift wherein targeted treatment of patients and lesions possessing high-risk atherosclerotic plaque characteristics may improve therapeutic precision and outcomes. Future studies addressing this approach now appear warranted.

ADDRESS FOR CORRESPONDENCE: Dr. James K. Min, Dalio Institute of Cardiovascular Imaging, New York-Presbyterian Hospital and Weill Cornell Medical College, 413 East 69th Street, Suite 108, New York, New York 10021. E-mail: jkm2001@med.cornell.edu.

PERSPECTIVES

COMPETENCY IN MEDICAL KNOWLEDGE: Although ACS are typically associated with stenotic coronary lesions, precursors of culprit lesions are commonly nonobstructive. HRP characteristics, plaque composition, and cross-sectional PB as assessed by coronary CTA can predict the development of ACS independently of stenosis severity and aggregate PB.

TRANSLATIONAL OUTLOOK: These characteristics of nonstenotic but high-risk coronary artery lesions should be investigated further in cohort studies and in prospective heart attack prevention trials.

REFERENCES

1. Schoenhagen P, Ziada KM, Kapadia SR, Crowe TD, Nissen SE, Tuzcu EM. Extent and direction of arterial remodeling in stable versus unstable coronary syndromes. Circulation 2000;101:598–603.

2. Virmani R, Burke AP, Farb A, Kolodgie FD. Pathology of the vulnerable plaque. J Am Coll Cardiol 2006;47:C13–8.

3. Yamagishi M, Terashima M, Awano K, et al. Morphology of vulnerable coronary plaque: insights from follow-up of patients examined by intravascular ultrasound before an acute coronary syndrome. J Am Coll Cardiol 2000;35:106–11.

4. Motoyama S, Sarai M, Harigaya H, et al. Computed tomographic angiography characteristics of atherosclerotic plaques subsequently resulting in acute coronary syndrome. J Am Coll Cardiol 2009;54:49–57.

5. Stone GW, Maehara A, Lansky AJ, et al. A prospective natural-history study of coronary atherosclerosis. N Engl J Med 2011;364:226–35.

6. Ehara S, Kobayashi Y, Yoshiyama M, et al. Spotty calcification typifies the culprit plaque in patients with acute myocardial infarction: an intravascular ultrasound study. Circulation 2004;110:3424–9.

7. Arbab-Zadeh A, Fuster V. The myth of the "vulnerable plaque": transitioning from a focus on individual lesions to atherosclerotic disease burden for coronary artery disease risk assessment. J Am Coll Cardiol 2015;65:846–55.

8. Budoff MJ, Dowe D, Jollis JG, et al. Diagnostic performance of 64-multidetector row coronary computed tomographic angiography for evaluation of coronary artery stenosis in individuals without known coronary artery disease: results from the prospective multicenter ACCURACY (Assessment by Coronary Computed Tomographic Angiography of Individuals Undergoing Invasive Coronary Angiography) trial. J Am Coll Cardiol 2008;52:1724–32.

9. Motoyama S, Ito H, Sarai M, et al. Plaque characterization by coronary computed tomography angiography and the likelihood of acute coronary events in mid-term follow-up. J Am Coll Cardiol 2015;66:337–46.

10. Puchner SB, Liu T, Mayrhofer T, et al. High-risk plaque detected on coronary CT angiography predicts acute coronary syndromes independent of significant stenosis in acute chest pain: results from the ROMICAT-II trial. J Am Coll Cardiol 2014;64:684–92.

11. Hoffmann U, Moselewski F, Nieman K, et al. Noninvasive assessment of plaque morphology and composition in culprit and stable lesions in acute coronary syndrome and stable lesions in stable angina by multidetector computed tomography. J Am Coll Cardiol 2006;47:1655–62.

12. Leipsic J, Abbara S, Achenbach S, et al. SCCT guidelines for the interpretation and reporting of coronary CT angiography: a report of the Society of Cardiovascular Computed Tomography Guidelines Committee. J Cardiovasc Comput Tomogr 2014;8:342–58.

13. Min JK, Dunning A, Lin FY, et al. Rationale and design of the CONFIRM (Coronary CT Angiography Evaluation for Clinical Outcomes: An International Multicenter) registry. J Cardiovasc Comput Tomogr 2011;5:84–92.

14. Mendis S, Thygesen K, Kuulasmaa K, et al. World Health Organization definition of myocardial infarction: 2008-09 revision. Int J Epidemiol 2011;40:139–46.

15. Austin PC. An introduction to propensity score methods for reducing the effects of confounding in observational studies. Multivariate Behav Res 2011;46:399–424.

16. Thygesen K, Alpert JS, Jaffe AS, et al. Third universal definition of myocardial infarction. Eur Heart J 2012;33:2551–67.

17. Abbara S, Blanke P, Maroules CD, et al. SCCT guidelines for the performance and acquisition of coronary computed tomographic angiography: a report of the Society of Cardiovascular Computed Tomography Guidelines Committee: endorsed by the North American Society for Cardiovascular Imaging (NASCI). J Cardiovasc Comput Tomogr 2016;10:435–49.

18. Park H-B, Lee BK, Shin S, et al. Clinical feasibility of 3D automated coronary atherosclerotic plaque quantification algorithm on coronary computed tomography angiography: comparison with intravascular ultrasound. Eur Radiol 2015;25:3073–83.

19. de Graaf MA, Broersen A, Kitslaar PH, et al. Automatic quantification and characterization of coronary atherosclerosis with computed tomography coronary angiography: cross-correlation with intravascular ultrasound virtual histology. Int J Cardiovasc Imaging 2013;29:1177–90.

20. Fihn SD, Gardin JM, Abrams J, et al. 2012 ACCF/AHA/ACP/AATS/PCNA/SCAI/STS guideline for the diagnosis and management of patients with stable ischemic heart disease: a report of the American College of Cardiology Foundation/American Heart Association Task Force on Practice Guidelines, and the American College of Physicians, American Association for Thoracic Surgery, Preventive Cardiovascular Nurses Association, Society for Cardiovascular Angiography and Interventions, and Society of Thoracic Surgeons. J Am Coll Cardiol 2012;60:e44–164.

21. Austin PC. The use of propensity score methods with survival or time-to-event outcomes: reporting measures of effect similar to those used in randomized experiments. Stat Med 2014;33:1242–58.

22. Lin DY, Wei LJ. The robust inference for the Cox proportional hazards model. J Am Stat Assoc 1989;84:1074–8.

23. Wei LJ, Lin DY, Weissfeld L. Regression analysis of multivariate incomplete failure time data by modeling marginal distributions. J Am Stat Assoc 1989;84:1065–73.

24. Libby P, Pasterkamp G. Requiem for the 'vulnerable plaque.'. Eur Heart J 2015:ehv349.

25. Maddox TM, Stanislawski MA, Grunwald GK, et al. Nonobstructive coronary artery disease and

risk of myocardial infarction. JAMA 2014;312:1754–63.

26. Ambrose JA, Tannenbaum MA, Alexopoulos D, et al. Angiographic progression of coronary artery disease and the development of myocardial infarction. J Am Coll Cardiol 1988;12:56–62.

27. Tian J, Ren X, Vergallo R, et al. Distinct morphological features of ruptured culprit plaque for acute coronary events compared to those with silent rupture and thin-cap fibroatheroma: a combined optical coherence tomography and intravascular ultrasound study. J Am Coll Cardiol 2014;63:2209–16.

28. Maurovich-Horvat P, Hoffmann U, Vorpahl M, Nakano M, Virmani R, Alkadhi H. The napkin-ring sign: CT signature of high-risk coronary plaques? J Am Coll Cardiol Img 2010;3:440–4.

29. Nakazato R, Otake H, Konishi A, et al. Atherosclerotic plaque characterization by CT angiography for identification of high-risk coronary artery lesions: a comparison to optical coherence tomography. Eur Heart J Cardiovasc Imaging 2015;16:373–9.

30. Boogers MJ, Broersen A, van Velzen JE, et al. Automated quantification of coronary plaque with computed tomography: comparison with intravascular ultrasound using a dedicated registration algorithm for fusion-based quantification. Eur Heart J 2012;33:1007–16.

31. Puri R, Nicholls SJ, Shao M, et al. Impact of statins on serial coronary calcification during atheroma progression and regression. J Am Coll Cardiol 2015;65:1273–82.

KEY WORDS acute coronary syndrome, atherosclerosis, clinical outcome, coronary artery disease, coronary computed tomography angiography

APPENDIX For additional information, including study organization and a list of participating site and investigators, supplemental data, and supplemental figures and tables, please see the online version of this paper.